Quantum properties of two-component two-sites Bose-Hubbard model

Author: Pere Mujal Torreblanca

Facultat de Física, Universitat de Barcelona, Diagonal 645, 08028 Barcelona, Spain.[*]

Advisors: Bruno Juliá-Díaz and Artur Polls

Abstract: This work contains a detailed analysis of the properties of the ground state of a two-component two-sites Bose-Hubbard model, which captures the physics of a binary mixture of Bose-Einstein condensates trapped in a double-well potential. The atom-atom interactions within each species and among the two species are taken as variable parameters while the hopping terms are kept fixed. To characterize the ground state we use observables such as the imbalance of population and its quantum uncertainty. The quantum many-body correlations present in the system are further quantified by studying the degree of condensation of each species, and the entanglement between the two species. The latter is measured by means of the Schmidt gap, the von Neumann entropy or the purity obtained after tracing out a part of the system. A number of relevant states are identified, e.g. Schrödinger catlike many-body states, in which the outcome of the population imbalance of both components is completely correlated, and other states with even larger von Neumann entropy which have a large spread in Fock space.

I. INTRODUCTION

Mixtures of Bose-Einstein condensates are interesting not only from a fundamental point of view, but also for their potential applications. Among the latter, the most prominent examples are found in quantum metrology [1, 2] and in quantum computation or quantum information processing, as discussed in Ref. [3]. A crucial ingredient is the possibility of generating entangled many-body states, e.g. Schrödinger catlike states. These type of states can be produced in a single component Bose-Einstein condensate trapped in a double-well potential, producing entanglement between the two-wells [4]. Interestingly, in the case of mixtures, having two different species allows us to explore a wider range of possibilities, e.g. having also entanglement between the different species.

Several procedures have been proposed to generate entangled many-body states in bosonic mixtures trapped in two wells. The first one is by dynamical generation, as in Ref. [3]. In such case, the system is prepared in a non-entangled state and the time evolution builds many-body correlations. A second procedure is to profit from Feshbach resonances to modify the atom-atom intra or interspecies interactions. In this thesis we will concentrate on this possibility.

The bosonic mixture trapped in a double-well potential will be described by means of a two-component two-site Bose-Hubbard model. Our goal is to explore the ground state properties of the system as a function of the atom-atom interactions, which are assumed to be tunable.

The thesis is organized as follows. First, in Sect. II we will describe the theoretical model and explain the procedure used to obtain the quantum many-body states.

Then, in Sect. III, we present the different magnitudes used to characterize the ground state properties of the system. The main ones are: 1) the imbalance of population between the wells, which can be measured experimentally in single component bosons; 2) the condensed fraction, which measures the degree of Bose-Einstein condensation of each component, and 3) entanglement measures, like von Neumann entropies of the subsystems after bipartition. Sections IV and V contain the main results. In Sect. IV we discuss the symmetric case, in which the bosons of the two species, A and B, have the same intraspecies interaction. In Sect. V we consider a more general case, in which the intraspecies interactions are not taken equal. Finally, in Sect. VI we provide a brief summary and conclusions.

II. DESCRIPTION OF THE MODEL

A mixture of two bosonic species with fixed number of particles, N_A particles of type A and N_B particles of type B, is considered trapped in a double well potential. The atom-atom interaction is assumed to be well approximated by a contact potential. Further, we consider only two single particle modes for each species [5]. Under this approximations we have the following second quantized Hamiltonian,

$$
\begin{aligned}
\hat{H} &= -J_A \left(\hat{a}_R^\dagger \hat{a}_L + \hat{a}_L^\dagger \hat{a}_R \right) - J_B \left(\hat{b}_R^\dagger \hat{b}_L + \hat{b}_L^\dagger \hat{b}_R \right) \\
&+ \frac{U_{AA}}{2} \left[\hat{n}_L^A(\hat{n}_L^A - 1) + \hat{n}_R^A(\hat{n}_R^A - 1) \right] \\
&+ \frac{U_{BB}}{2} \left[\hat{n}_L^B(\hat{n}_L^B - 1) + \hat{n}_R^B(\hat{n}_R^B - 1) \right] \\
&+ U_{AB} \left(\hat{n}_L^A \hat{n}_L^B + \hat{n}_R^A \hat{n}_R^B \right) \\
&- \epsilon \left(\hat{n}_L^B - \hat{n}_R^B \right),
\end{aligned} \tag{1}
$$

---

[*]Electronic address: `peremujal@gmail.com`

where $[\hat{a}_i^\dagger, \hat{a}_j] = \delta_{i,j}$, $[\hat{b}_i^\dagger, \hat{b}_j] = \delta_{i,j}$, $\hat{n}_i^A = \hat{a}_i^\dagger \hat{a}_i$, $\hat{n}_i^B = \hat{b}_i^\dagger \hat{b}_i$ and $i, j = L, R$ (L associated with the left site and R with the right site). The action of the creation and annihilation operators on the Fock basis reads, for instance for L,

$$\hat{a}_L^\dagger |n_L^A, n_R^A, n_L^B, n_R^B\rangle = \sqrt{n_L^A + 1} |n_L^A + 1, n_R^A, n_L^B, n_R^B\rangle,$$

$$\hat{b}_L^\dagger |n_L^A, n_R^A, n_L^B, n_R^B\rangle = \sqrt{n_L^B + 1} |n_L^A, n_R^A, n_L^B + 1, n_R^B\rangle,$$

$$\hat{a}_L |n_L^A, n_R^A, n_L^B, n_R^B\rangle = \sqrt{n_L^A} |n_L^A - 1, n_R^A, n_L^B, n_R^B\rangle,$$

$$\hat{b}_L |n_L^A, n_R^A, n_L^B, n_R^B\rangle = \sqrt{n_L^B} |n_L^A, n_R^A, n_L^B - 1, n_R^B\rangle. \quad (2)$$

The strength of the intra, AA and BB, and interspecies, AB, interaction is given by the parameter U_{AA}, U_{BB} and U_{AB}, respectively. Within our sign convention, positive and negative values of $U_{\alpha\beta}$ correspond to repulsive and attractive interactions, respectively. The hopping parameters J_A and J_B can in principle be varied by raising or lowering the potential barrier between the two wells. A small bias term, $0 < \epsilon \ll J_A, J_B$, ensures the breaking of left-right symmetry and also $A - B$ symmetry. In our case it has been chosen to be energetically favourable to have B particles on the L site. We define the parameters $\Lambda_A \equiv N_A U_{AA}/J_A$, $\Lambda_B \equiv N_B U_{BB}/J_B$ and $\Lambda_{AB} \equiv N_A U_{AB}/J_A = N_B U_{AB}/J_B$.

To diagonalize the Hamiltonian we consider the following Fock basis,

$$|k_A, k_B\rangle \equiv |N_A - k_A, k_A\rangle |N_B - k_B, k_B\rangle, \quad (3)$$

where $k_A = 0, ..., N_A$ and $k_B = 0, ..., N_B$ and thus the dimension of the Hilbert space is $(N_A + 1)(N_B + 1)$. The state $|k_A, k_B\rangle$ is the one having k_A bosons of type A on the right and k_B bosons of type B on the right.

Therefore, the matrix elements of the Hamiltonian are,

$$
\begin{aligned}
\langle k_A', k_B'| \ \hat{H} \ |k_A, k_B\rangle = \\
\frac{U_{AA}}{2}[(N_A - k_A)(N_A - k_A - 1) \\
+ \quad k_A(k_A - 1)]\delta_{k_A,k_A'}\delta_{k_B,k_B'} \\
+ \quad \frac{U_{BB}}{2}[(N_B - k_B)(N_B - k_B - 1) \\
+ \quad k_B(k_B - 1)]\delta_{k_A,k_A'}\delta_{k_B,k_B'} \\
- \quad J_A\sqrt{(N_A - k_A)(k_A + 1)}\,\delta_{k_A+1,k_A'}\delta_{k_B,k_B'} \\
- \quad J_A\sqrt{k_A(N_A + 1 - k_A)}\,\delta_{k_A-1,k_A'}\delta_{k_B,k_B'} \\
- \quad J_B\sqrt{(N_B - k_B)(k_B + 1)}\,\delta_{k_A,k_A'}\delta_{k_B+1,k_B'} \\
- \quad J_B\sqrt{k_B(N_B + 1 - k_B)}\,\delta_{k_A,k_A'}\delta_{k_B-1,k_B'} \\
+ \quad U_{AB}[(N_A - k_A)(N_B - k_B) \\
+ \quad k_A k_B]\delta_{k_A,k_A'}\delta_{k_B,k_B'} \\
- \quad \epsilon(N_B - 2k_B)\delta_{k_A,k_A'}\delta_{k_B,k_B'}. \quad (4)
\end{aligned}
$$

Diagonalizing the Hamiltonian matrix introduced in (4) using the routine *gsl_eigen_symmv* from *GNU Scientific Library*, the energy spectrum is obtained numerically and the ground state is found in different situations.

III. GROUND STATE PROPERTIES

A. Spectral decomposition and degeneracy

The ground state of the system $|\Psi_0\rangle$, can be expressed in the Fock basis as

$$|\Psi_0\rangle = \sum_{k_A=0}^{N_A} \sum_{k_B=0}^{N_B} C_{k_A,k_B} |k_A, k_B\rangle. \quad (5)$$

Since it is an eigenvector of the Hamiltonian it satisfies $\hat{H} |\Psi_0\rangle = E_0 |\Psi_0\rangle$, with E_0 the energy of the ground state. The first excited state $|\Psi_1\rangle$ satisfies $\hat{H} |\Psi_1\rangle = E_1 |\Psi_1\rangle$. Degeneracy will occur when at least two different eigenstates have the same energy. For this reason, the difference

$$\Delta E_{1,0} \equiv E_1 - E_0, \quad (6)$$

determines whether the ground state is degenerate or not.

B. Population imbalance

The population imbalance z_i, with $i = A, B$, for a given arbitrary state of the system $|\Psi\rangle$, is defined as the expectation value

$$z_i \equiv \frac{1}{N_i} \langle\Psi| \hat{n}_L^i - \hat{n}_R^i |\Psi\rangle. \quad (7)$$

For a state with all particles of type $A(B)$ on the left site $z_{A(B)}$ is 1, while if all the particles are on the right site its value is -1. This quantity is zero in the case of equal population of particles of a given type in the two sites. We can also compute the dispersion of z_i

$$\sigma_z^i \equiv \sqrt{\langle\Psi| \left(\frac{\hat{n}_L^i - \hat{n}_R^i}{N_i}\right)^2 |\Psi\rangle - \left(\langle\Psi| \frac{\hat{n}_L^i - \hat{n}_R^i}{N_i} |\Psi\rangle\right)^2}. \quad (8)$$

Particularly for the ground state $|\Psi_0\rangle$ using its spectral decomposition (5) we can express the population imbalance (7) for each component of the mixture as

$$z_i = \sum_{k_A=0}^{N_A} \sum_{k_B=0}^{N_B} |C_{k_A,k_B}|^2 \frac{N_i - 2k_i}{N_i} \quad (9)$$

and also the corresponding dispersion (8) as

$$\sigma_z^i = \left[\sum_{k_A=0}^{N_A} \sum_{k_B=0}^{N_B} |C_{k_A,k_B}|^2 \left(\frac{N_i - 2k_i}{N_i}\right)^2 - \left(\sum_{k_A=0}^{N_A} \sum_{k_B=0}^{N_B} |C_{k_A,k_B}|^2 \frac{N_i - 2k_i}{N_i} \right)^2 \right]^{1/2}. \quad (10)$$

C.   Degree of condensation

The degree of condensation of each of the species in the ground state is characterized using the one-body density matrix for each component

$$\rho_{i,j}^A \equiv \frac{1}{N_A} \langle \Psi_0 | \, \hat{a}_i^\dagger \hat{a}_j \, | \Psi_0 \rangle , \qquad (11)$$

$$\rho_{i,j}^B \equiv \frac{1}{N_B} \langle \Psi_0 | \, \hat{b}_i^\dagger \hat{b}_j \, | \Psi_0 \rangle , \qquad (12)$$

where in both equations (11) and (12) $i, j = L, R$.

Diagonalizing $\rho^{A(B)}$ we obtain its eigenvalues $n_1^{A(B)}$ and $n_2^{A(B)}$ normalized to unity, which correspond to the condensed fraction in the macro-occupied single-particle eigenstate of the one-body density matrix $|\phi_1^{A(B)}\rangle$ and $|\phi_2^{A(B)}\rangle$ respectively.

The eigenvalues fulfill $n_1^{A(B)} + n_2^{A(B)} = 1$ and, by definition, $0 \leq n_2^{A(B)} \leq n_1^{A(B)}$. In the particular case when $n_1^{A(B)} = 1$, all the bosons of type $A(B)$ populate the same single particle state $|\phi_1^{A(B)}\rangle$ and the state of the subsystem of bosons of type $A(B)$ can be written as a product state $|\Phi_1^{A(B)}\rangle \equiv |\phi_1^{A(B)}\rangle^{\otimes N_{A(B)}}$.

D.   Partial traces, purity and entanglement

The density matrix associated with the ground state $|\Psi_0\rangle$, that describes completely the state of the total system formed by the two types of particles, is

$$\hat{\rho}_0 \equiv |\Psi_0\rangle \langle \Psi_0| . \qquad (13)$$

This matrix has dimension $(N_A + 1)(N_B + 1)$. If we are interested in only one part of the system, for instance the type $A(B)$ bosons, we can obtain the state for this subsystem taking the partial trace with respect to $B(A)$ of the matrix $\hat{\rho}_0$. The state of type $A(B)$ bosons then would be described by $\hat{\rho}_0^{A(B)}$, that is

$$\hat{\rho}_0^{A(B)} \equiv \mathrm{Tr}_{B(A)}[\hat{\rho}_0], \qquad (14)$$

which has dimension $(N_{A(B)} + 1)$.

In general, after tracing out part of the system, the state of the remaining subsystem is a mixed state. In order to determine if $\hat{\rho}_0^{A(B)}$ is a pure state or not and its degree of purity, the trace of this matrix squared, $P_{A(B)}$, is computed,

$$P_{A(B)} \equiv \mathrm{Tr}[(\hat{\rho}_0^{A(B)})^2]. \qquad (15)$$

When the state of each subsystem is a pure state we obtain $P_{A(B)} = 1$. In this case the ground state is a product state $|\Psi_0\rangle = |\Psi_0^A\rangle \, |\Psi_0^B\rangle$ and there is no entanglement between A and B. Otherwise, when $P_{A(B)} \neq 1$, the ground state is not a product state, $|\Psi_0\rangle \neq |\Psi_0^A\rangle \, |\Psi_0^B\rangle$, and $P_{A(B)}$ satisfies $\frac{1}{N_{A(B)}+1} \leq P_{A(B)} < 1$, now having entanglement between A and B with completely entangled subsystems for the case $\hat{\rho}_0^{A(B)} = \frac{1}{N_{A(B)}+1}\mathbb{I}$.

E.   Entropy and Schmidt gap

The von Neumann entropy of the state of each subsystem is computed diagonalizing

$$\hat{\rho}_0^{A(B)} = \sum_{i=0}^{N_{A(B)}} \lambda_i^{A(B)} |\lambda_i^{A(B)}\rangle \langle \lambda_i^{A(B)}|, \qquad (16)$$

to obtain its eigenvalues $\lambda_i^{A(B)}$, considering $\lambda_0^{A(B)} \geq \lambda_1^{A(B)} \geq ... \geq \lambda_{N_{A(B)}}^{A(B)}$. As the density matrix $\hat{\rho}_0^{A(B)}$ is normalized, $\mathrm{Tr}[\hat{\rho}_0^{A(B)}] = 1$, the eigenvalues satisfy $\sum_{i=0}^{N_{A(B)}} \lambda_i^{A(B)} = 1$. In order to calculate the entropy $S_{A(B)}$ we use the definition

$$S_{A(B)} \equiv -\mathrm{Tr}\left[\hat{\rho}_0^{A(B)} \log \hat{\rho}_0^{A(B)} \right] = - \sum_{i=0}^{N_{A(B)}} \lambda_i^{A(B)} \log \lambda_i^{A(B)}, \qquad (17)$$

where if a $\lambda_i^{A(B)} = 0$, the corresponding term is considered to be zero and it is not added to the sum. The entropy has a minimum value equal to zero when all the $\lambda_i^{A(B)} = 0$ except $\lambda_0^{A(B)} = 1$ and then the state is pure. Its maximum value, $S_{max}^{A(B)} = \log(N_{A(B)} + 1)$, is reached when $\lambda_0 = \lambda_1^{A(B)} = ... = \lambda_{N_{A(B)}}^{A(B)} = \frac{1}{N_{A(B)}+1}$ and in this case we have the maximum entanglement situation (discussed previously) which means that each subsystem is in a mixed state.

The Schmidt gap is defined as the difference between the two largest eigenvalues of the density matrix,

$$\Delta\lambda^{A(B)} \equiv \lambda_0^{A(B)} - \lambda_1^{A(B)}, \qquad (18)$$

and also distinguishes between having pure states and no entanglement between the A and B when $\Delta\lambda^{A(B)} = 1$ and totally entangled subsystems and mixed states for part A and B if $\Delta\lambda^{A(B)} = 0$.

IV.   SAME INTRASPECIES INTERACTION

In this section we present our results for the case in which the intraspecies interaction is the same for both species. We discuss how the properties of the system change as we vary the interspecies one, U_{AB}. The non

interacting case between different type bosons ($U_{AB} = 0$) is equivalent to having two independent, but different because of bias in equation (1), single-component Bose-Einstein condensate in a double-well, which is studied in [6] and [7]. In terms of our parameters, $N_A = N_B$, $U_{AA} = U_{BB}$, $J_A = J_B$ and $U_{AB} \neq U_{AA}$. Now for simplicity we define $\Lambda \equiv \Lambda_A = \Lambda_B$ and also $J \equiv J_A = J_B$. In our numerical calculations $N_A = N_B = 20$, $J = 20$ and $\epsilon/J = 10^{-10}$. Thus, the Hamiltonian is a 441×441 matrix, which is diagonalized for different values of Λ and Λ_{AB}. We organize the section as follows. First we discuss the spectral decomposition of the ground state depending on the character of the intraspecies interaction. Second, we study the condensed fraction and entanglement properties as a function of Λ and Λ_{AB}.

A.   Repulsive intraspecies interaction

In this case we have $\Lambda > 0$, i.e. atoms of each species repel each other. We can consider three situations, $\Lambda_{AB} > 0$, $\Lambda_{AB} < 0$ and $\Lambda_{AB} = 0$.

$\mathbf{\Lambda_{AB} > 0}$. In this case, particles of different type do not want to be at the same site. For $\Lambda_{AB} \gg \Lambda \gg 1$, this can be achieved with all type A bosons on the right site and type B bosons on the left site, or similarly with type B bosons on the right and type A bosons on the left site. These two states are degenerate in this limit and, therefore, any superposition of these states, $|\Psi_0\rangle = \alpha |N_A, 0\rangle + \beta |0, N_B\rangle$, with $|\alpha|^2 + |\beta|^2 = 1$, has the same energy. This degeneracy is broken by the bias term introduced in the Hamiltonian, and since the bias has been chosen to be energetically favourable to have B particles on the left site, the ground state is $|\Psi_0\rangle = |N_A, 0\rangle$. This limiting case, obtained for $\Lambda_{AB} \gg \Lambda \gg 1$, can help to understand the numerical results. For instance in Fig. 1(g) we present the spectral decomposition of the state obtained for $\Lambda_{AB} = 10$ and $\Lambda = 4$. The ground state is seen to be close to the $|N_A, 0\rangle$. As the Λ_{AB} is decreased, the bias term is not large enough to localize the state and the ground state is closer to the linear combination $\frac{1}{\sqrt{2}}(|N_A, 0\rangle \pm |0, N_B\rangle)$, see Fig. 1(f).

$\mathbf{\Lambda_{AB} < 0}$.   Attractive interaction between different bosons, will make all of them be at the same site despite the repulsion between same type bosons because now we consider the regime where $-\Lambda_{AB} \gg \Lambda \gg 1$. There is degeneracy in this case, too. Bosons can be all together on the right, $|\Psi_0\rangle = |N_A, N_B\rangle$, or on the left $|\Psi_0\rangle = |0, 0\rangle$, or also any superposition of the two situations $|\Psi_0\rangle = \alpha |N_A, N_B\rangle + \beta |0, 0\rangle$, with $|\alpha|^2 + |\beta|^2 = 1$. Again, the bias breaks the symmetry and in this case selects the state $|\Psi_0\rangle = |0, 0\rangle$ because type B bosons are on the left site in this one. The numerical results do agree with these arguments. For $\Lambda_{AB} = -10$ the ground state is close to the state $|0, 0\rangle$, see Fig. 1(a). For $\Lambda_{AB} = -8$ the bias does not localize the state and the ground state is close to a linear combination $\frac{1}{\sqrt{2}}(|0, 0\rangle \pm |N_A, N_B\rangle)$.

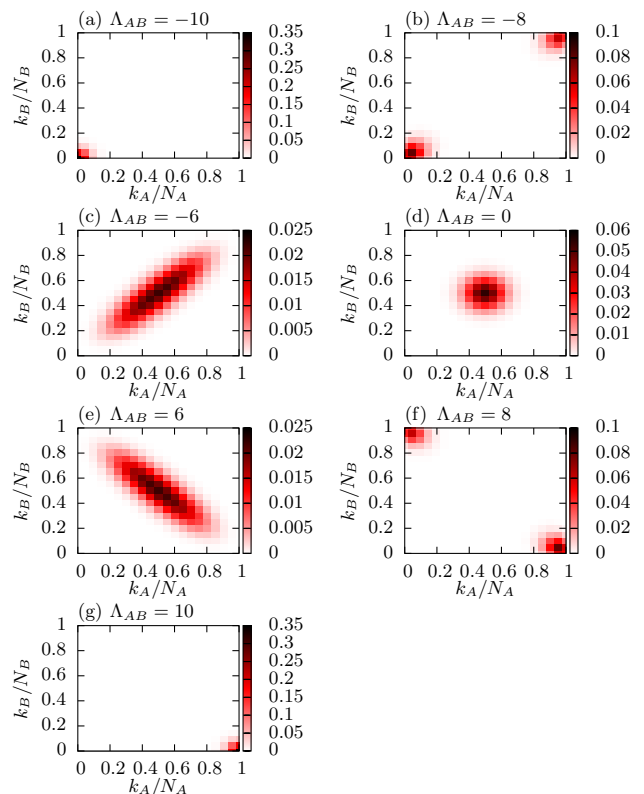For $\mathbf{\Lambda_{AB} = 0}$, the system is equivalent to having two

FIG. 1: Spectral decomposition of the ground state, $|C_{k_A, k_B}|^2$, for repulsive intraspecies interaction ($\Lambda > 0$), plotted for different values of Λ_{AB}. We observe the transition from (a), a regime dominated by the attraction between the different species to a regime (g) dominated by the repulsion between species A and B, going through intermediate regimes in the panels (b) to (f). For all panels $\Lambda = 4$, $N_A = N_B = 20$, $J = 20$ and $\epsilon/J = 10^{-10}$.

independent bosonic Josephson junctions. The ground state of the full system is the direct product of the ground state of each subsystem. Thus, we obtain a left-right $A - B$ symmetric ground state (see Fig. 1(d)). This type of state would be binomial for each component [6] for $\Lambda = 0$. For $\Lambda > 0$ it becomes squeezed. In the limit case when $|\Lambda| \gg 1$ it tends to $|\Psi_0\rangle = \left|\frac{N_A}{2}, \frac{N_B}{2}\right\rangle$.

When the bias does not play a role, i.e. when $\epsilon \ll \Delta E_{1,0}$, the Hamiltonian has left-right and $A - B$ symmetries so in this situation its eigenstates have these symmetries too. Therefore, catlike states appear for $\Lambda_{AB} < 0$ as well as for $\Lambda_{AB} > 0$. In both cases, the ground state is quasi-degenerate with the first excited state. Without bias in the Λ_{AB} dominated regime we have for attractive intraspecies interaction $|\Psi_0\rangle = \frac{1}{\sqrt{2}}(|N_A, N_B\rangle \pm |0, 0\rangle)$ and for the repulsive case $|\Psi_0\rangle = \frac{1}{\sqrt{2}}(|N_A, 0\rangle \pm |0, N_B\rangle)$. This is mainly what is found in Fig. 1(b) and Fig. 1(f) respectively. For $|\Lambda_{AB}|$ small enough, the two peaks merge and form a broadened peak which has its tails pointing to the previous corresponding two peaks (see Figs. 1(c) and 1(e)) and becomes narrow when $|\Lambda_{AB}|$ decreases un-

	$\Lambda > 0$	$\Lambda < 0$
$\Lambda_{AB} > 0$	$(1/\sqrt{2})(|N_A, 0\rangle \pm |0, N_B\rangle)$	$(1/\sqrt{2})(|N_A, 0\rangle \pm |0, N_B\rangle)$
$\Lambda_{AB} = 0 \ (|\Lambda| \gg 0)$	$|N_A/2, N_B/2\rangle$	$(1/2)(|N_A, N_B\rangle + |N_A, 0\rangle + |0, N_B\rangle + |0, 0\rangle)$
$\Lambda_{AB} < 0$	$(1/\sqrt{2})(|0, 0\rangle \pm |N_A, N_B\rangle)$	$(1/\sqrt{2})(|0, 0\rangle \pm |N_A, N_B\rangle)$

TABLE I: Ground state for the case $|\Lambda_{AB}| \gg |\Lambda|$ in absence of tunnelling ($\Lambda \gg 1$) and in absence of bias depending on the character of inter and intraspecies interaction.

til $\Lambda_{AB} = 0$.

B.   Attractive intraspecies interaction

As in previous subsection A, we can distinguish three cases. The repulsive case for different particles, when $\Lambda_{AB} > 0$, the attractive one when $\Lambda_{AB} < 0$ and the non interacting for $\Lambda_{AB} = 0$.

$\mathbf{\Lambda_{AB} > 0}$. Here the repulsion between different type bosons and the attraction between same type bosons are not competing, in the sense that both effects can be easily fulfilled simultaneously, which did not happen in the two first limits discussed in subsection A. Particles of the same type want to be together and separated from the other type ones. The states that accomplish this in absence of tunnelling are $|\Psi_0\rangle = |N_A, 0\rangle$, $|\Psi_0\rangle = |0, N_B\rangle$ and their superposition $|\Psi_0\rangle = \alpha |N_A, 0\rangle + \beta |0, N_B\rangle$, with $|\alpha|^2 + |\beta|^2 = 1$. The bias breaks the symmetry towards $|\Psi_0\rangle = |N_A, 0\rangle$ (see Fig. 2(g)). Notice that this argument also holds for the repulsive-repulsive case (repulsion between same and different type of bosons).

$\mathbf{\Lambda_{AB} < 0}$. This is the attractive-attractive case where, in absence of tunnelling, it is clear that all the bosons will be at the same site. Now the states expected are the same as in the regime of domination of attractive interaction between different bosons and repulsive interaction between same bosons. The difference in this case is that the effects of Λ and Λ_{AB} go in the same direction. The ground state candidates are $|\Psi_0\rangle = |N_A, N_B\rangle$, $|\Psi_0\rangle = |0, 0\rangle$ and, as before, their superposition $|\Psi_0\rangle = \alpha |N_A, N_B\rangle + \beta |0, 0\rangle$, with $|\alpha|^2 + |\beta|^2 = 1$, with the bias breaking the symmetry and selecting the state $|\Psi_0\rangle = |0, 0\rangle$ (see Fig. 2(a)).

Here, we also have the catlike states described in the previous section as it is shown in Figs. 2(b) and 2(f). However, the ground state for $\mathbf{\Lambda_{AB} = 0}$ is a different one (see Fig. 2(d)) and thus the intermediate states too (see Fig. 2(c) and 2(e)). The ground state for zero intraspecies interaction is degenerate not only with the first excited state but also with the second, the third and the fourth. Looking only in one type of bosons we have in these conditions a left-right catlike state [6], so here we see this for both components at the same time. Each catlike state for each species is degenerate, what means that the ground state of the whole system is the degeneracy of $|\Psi_0\rangle = \frac{1}{2}(|N_A, N_B\rangle + |N_A, 0\rangle + |0, N_B\rangle + |0, 0\rangle)$, $|\Psi_0\rangle = \frac{1}{2}(|N_A, N_B\rangle - |N_A, 0\rangle - |0, N_B\rangle + |0, 0\rangle)$, $|\Psi_0\rangle = \frac{1}{2}(|N_A, N_B\rangle - |N_A, 0\rangle + |0, N_B\rangle - |0, 0\rangle)$ and $|\Psi_0\rangle =$
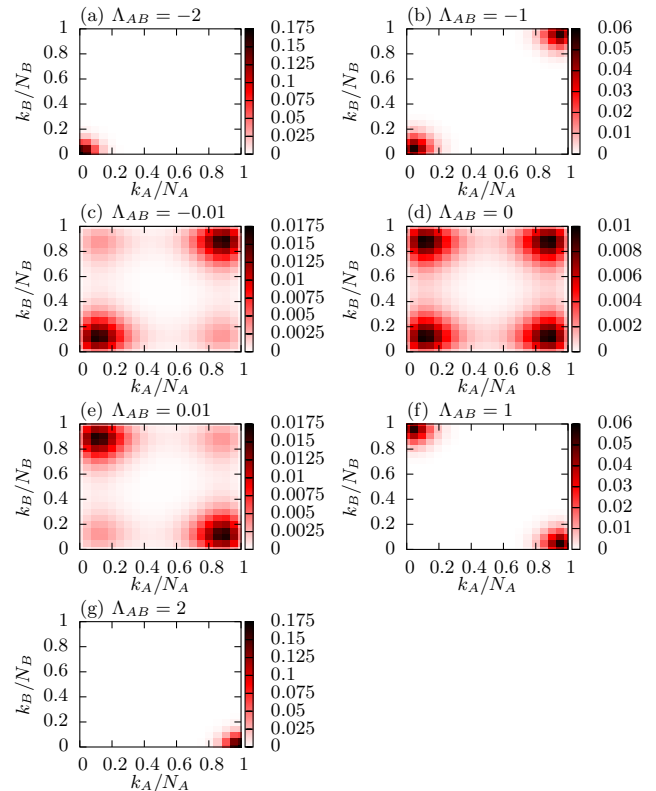

FIG. 2: Spectral decomposition of the ground state, $|C_{k_A, k_B}|^2$, for attractive intraspecies interaction ($\Lambda < 0$), plotted for different values of Λ_{AB}. We observe the transition from (a), a regime dominated by the attraction between the different species to a regime (g) dominated by the repulsion between species A and B, going through intermediate regimes in the panels (b) to (f). For all panels $\Lambda = -3$, $N_A = N_B = 20$, $J = 20$ and $\epsilon/J = 10^{-10}$.

$\frac{1}{2}(|N_A, N_B\rangle + |N_A, 0\rangle - |0, N_B\rangle - |0, 0\rangle)$. As occurred before, the tunnelling mixes the four states and for finite Λ we obtain states close to these ones but with a finite width in the Fock space, Fig. 2(c,d,e).

In Table I we summarize the ground state in the interaction dominating regime.

C.   Condensed fractions and entanglement properties

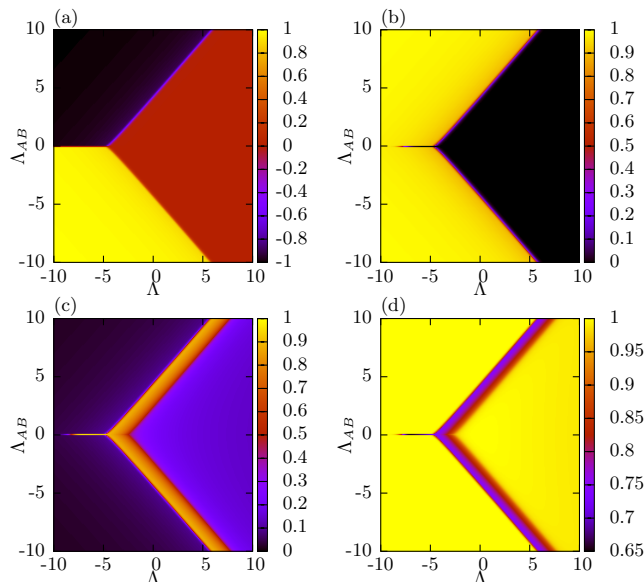Up to now, we have mainly discussed the spectral structure of the ground states for different values of Λ and

FIG. 3: For same intraspecies interaction, (a) population imbalance of the ground state, z_A, for type A bosons. The particles of this type are all on the left $z_A = 1$ (yellow), all on the right $z_A = -1$ (black) and $z_A = 0$ (red). (b) Population imbalance of the ground state, z_B, for type B bosons. The particles of this type are all on the left $z_B = 1$ (yellow) and $z_B = 0$ (black). (c) Dispersion of population imbalance of the ground state for type B bosons, σz_B, depending on the characteristic parameters Λ and Λ_{AB}. (d) Condensed fraction n_1^B of the ground state corresponding to the highest eigenvalue of the one-body density matrix as a function of Λ and Λ_{AB}. For $\Lambda_{AB} = 0$ (non interacting case between different type bosons) the results obtained in [6] are reproduced. For all panels $N_A = N_B = 20$, $J = 20$ and $\epsilon/J = 10^{-10}$.
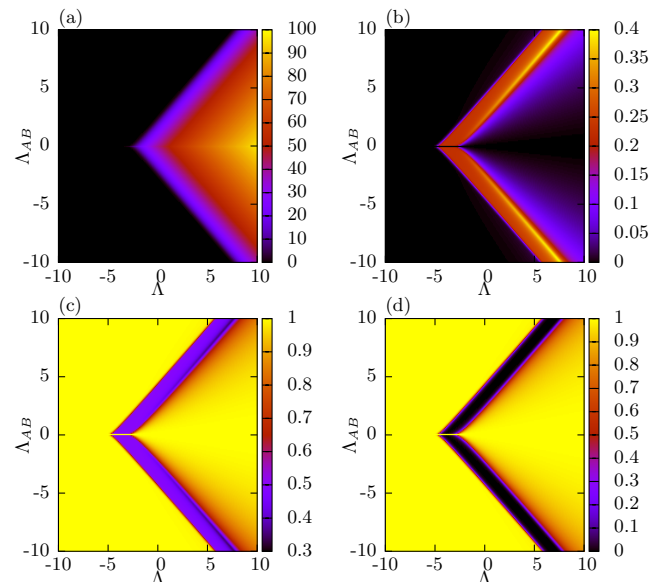
FIG. 4: For same intraspecies interaction, (a) difference between the energy of the first excited state and the ground state $\Delta E_{1,0}$ depending on Λ and Λ_{AB}. The black region is where there is degeneracy. (b) Von Neumann entropy of the ground state for subsystem $A(B)$, $S_{A(B)}$ normalized to its maximum value. (c) Trace of the density matrix squared of the ground state for subsystem $A(B)$, $P_{A(B)}$. (d) Schmidt gap of the ground state for subsystem $A(B)$, $\Delta\lambda^{A(B)}$. For all panels $N_A = N_B = 20$, $J = 20$ and $\epsilon/J = 10^{-10}$.

Λ_{AB}. Starting from the interaction dominated cases, we have understood the Fock space structure of the ground state found in our numerical diagonalization. In particular, we have identified regimes in which ground state quasidegeneracies and many-body fragmentation is expected to appear. In this section, we will characterize the condensation of the two ultracold atomic clouds and the entanglement between the two species.

First, let us provide a global picture and consider the population imbalance of the ground state for the A and B species as a function of Λ and Λ_{AB}. The main difference between the two species is found in the attractive intraspecies interaction case, as seen by comparing panels (a) and (b) of Fig. 3. This is due to the bias term which breaks explicitly the $A - B$ symmetry, which in the interaction dominated regime localizes the B atoms on the left and the A atoms on the right.

The population imbalance only provides an average information, which does not allow to differentiate for instance two very different quantum states, e.g. Fig. 1(b) and Fig. 1(d). Both of these states have a zero population imbalance, but the structure in Fock space is completely different. For instance, it can be inferred directly

from the figure that the two states should have a very different quantum uncertainty for the imbalance of population. This means for instance the following. If one prepares the system in the state shown in Fig 1(b) and measures the populations, the outcome of the measurements will be very polarized, i.e. almost all particles of each species will be found on the same well in each experiment. On average, however, we should find an average of population equal to zero. In contrast, in the state depicted in Fig. 1(d), the outcome of each individual experiment will almost never be too polarized, finding outcomes where a similar number of particles of each species is found in each well. These two states can be discriminated by means of the dispersion of the population imbalance σ_z, Eq. (10), which is depicted in Fig. 3(c).

In Fig. 3(c) we consider the dispersion of the population imbalance for the B atoms. The sharp lines delimiting the different population imbalance regions seen in Fig. 3(b) are replaced by broad transition regions in Fig. 3(c). This is a quantal effect, similar to the transition observed in the single component case [6]. As occurred in the single component case, in the transition regions the many-body state is very fragmented. As seen in Fig. 3(d), the B component is almost fully condensed for all values of Λ and Λ_{AB} except for the transition regions, where the condensed fraction falls below 0.7. These fragmented states are for instance the ones in Fig. 1(b,c,e,f).
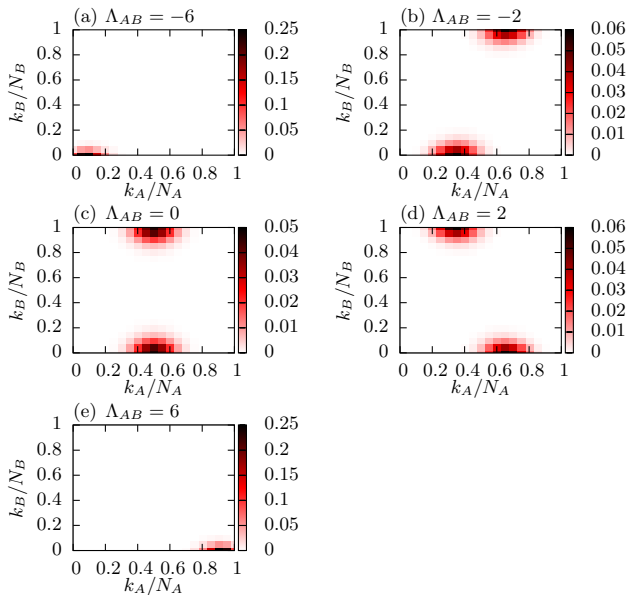
FIG. 5: Spectral decomposition of the ground state, $|C_{k_A,k_B}|^2$, plotted for different values of Λ_{AB}. Here there is repulsion between A ($\Lambda_A > 0$) and attraction between B type bosons ($\Lambda_B < 0$). We observe the transition from (a), a regime dominated by the attraction between the different species to a regime (e) dominated by the repulsion between species A and B, going through intermediate regimes in the panels (b) to (d). For all panels $\Lambda_A = 4$, $\Lambda_B = -5$, $N_A = N_B = 20$, $J = 20$ and $\epsilon/J = 10^{-10}$.

As explained above, in certain limits the ground state becomes degenerate with the first excited state. In Fig. 4(a) we depict $\Delta E_{1,0}$. Small degeneracies are not seen in the figure, and thus, for instance, the localisation due to the bias is not reflected in the figure. For $\Lambda < 0$ the ground state is mostly degenerate. Gapped ground states are found for repulsive intraspecies interactions and also in the transition regions.

The entanglement between the two subsystems is characterized by the purity, von Neumann entropy and Schmidt gap of the density matrix after tracing out a certain subsystem. The Schmidt gap provides a broad picture of presence of entanglement, see Fig 4(d). As it only involves the difference between the two largest Schmidt coefficients, it does not differentiate between different entangled states, for instance, it cannot discriminate between a catlike state, Fig. 1(b) and a broadened peak Fig. 1(c). These two states can be told apart by computing the von Neumann entropy, Fig. 4(b). In this case, the broadened peak has a larger number of sizeable Schmidt coefficients than in the catlike case, and thus shows as a maximum of the von Neumann entropy, in yellow inside the transition region. A similar discussion can be made with the states in Fig. 1(e) and (f), which again have a similar Schmidt gap but different von Neumann entropy. The purity, shown in Fig. 4(c) provides a very similar global picture as the Schmidt gap.
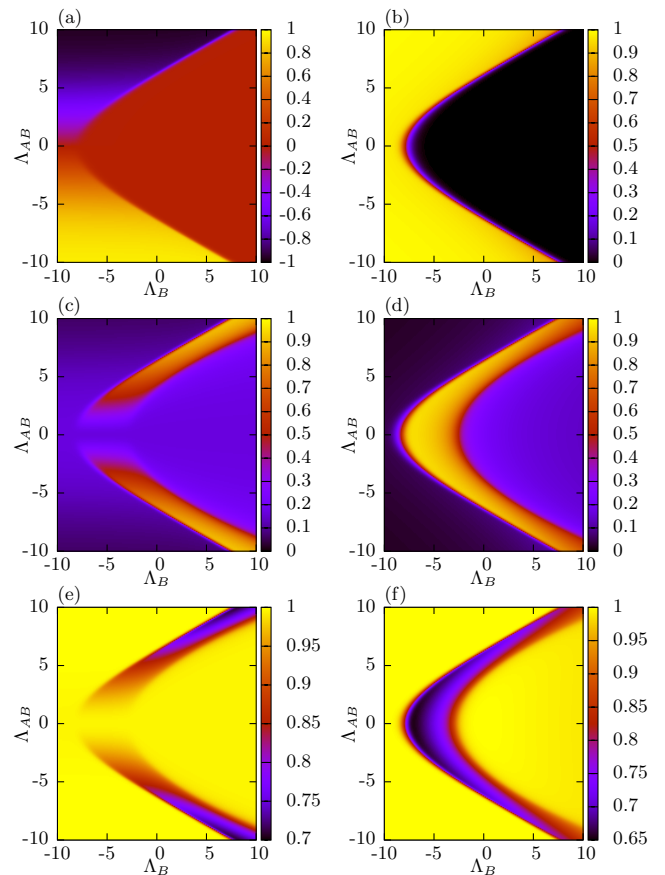

FIG. 6: For different intraspecies interaction and fixing $\Lambda_A > 0$ and varying Λ_B and Λ_{AB}, population imbalance of the ground state, z_A, (a) for type A and (b) for type B bosons, z_B. Dispersion of population imbalance of the ground state for each specie, (c) σz_A and (d) σz_B. Condensed fraction of the ground state corresponding to the highest eigenvalue of the one-body density matrix for each type, (e) n_1^A and (f) n_1^B. For all panels $\Lambda_A = 4$, $N_A = N_B = 20$, $J = 20$ and $\epsilon/J = 10^{-10}$.

V. DIFFERENT INTRASPECIES INTERACTION

In this section we will study the case $U_{AA} \neq U_{BB}$ with the same number of particles for each species, $N_A = N_B$ and as before $J \equiv J_A = J_B$ with $J/\epsilon = 10^{10}$. We consider a fixed value of Λ_A for repulsive ($\Lambda_A > 0$) and attractive interaction ($\Lambda_A < 0$) and allow for variations of the parameters Λ_B and Λ_{AB}.

A. Repulsive intraspecies interaction Λ_A

We consider bosons of type A with repulsive intraspecies interaction mixed with bosons of type B. In this case, we will allow for a variation of the interactions of the B bosons with themselves (Λ_B) and with the other species (Λ_{AB}).
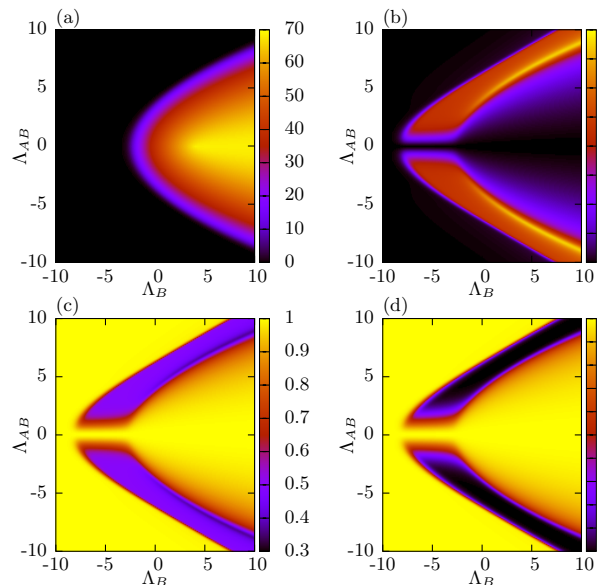
FIG. 7: For different intraspecies interaction and fixing $\Lambda_A > 0$ and varying Λ_B and Λ_{AB}, (a) difference between the energy of the first excited state and the ground state $\Delta E_{1,0}$. (b) Von Neumann entropy of the ground state for subsystem $A(B)$, $S_{A(B)}$ normalized to its maximum value. (c) Trace of the density matrix squared of the ground state for subsystem $A(B)$, $P_{A(B)}$. (d) Schmidt gap of the ground state for subsystem $A(B)$, $\Delta\lambda^{A(B)}$. For all panels $\Lambda_A = 4$, $N_A = N_B = 20$, $J = 20$ and $\epsilon/J = 10^{-10}$.

FIG. 8: Spectral decomposition of the ground state, $|C_{k_A,k_B}|^2$, plotted for different values of Λ_{AB}. Here there is attraction between A ($\Lambda_A < 0$) and repulsion between B type bosons ($\Lambda_B > 0$). We observe the transition from (a), a regime dominated by the attraction between the different species to a regime (e) dominated by the repulsion between species A and B, going through intermediate regimes in the panels (b) to (d). For all panels $\Lambda_A = -4$, $\Lambda_B = 5$, $N_A = N_B = 20$, $J = 20$ and $\epsilon/J = 10^{-10}$.

Here we have found mainly the same type of states and transitions described in section IV. There are, however, new states and different behaviour for each type of bosons. For instance, for $\Lambda_B > 0$ the states that are found are the ones of Fig. 1 but appearing for different values of Λ_{AB}. For this reason we focus on the case of having $\Lambda_B < 0$ as it is shown in Fig. 5. In the extreme cases (see Figs. 5(a) and 5(e)), the states are similar to the ones in Figs. 1(a) and 1(g). In these cases the physics is dominated by Λ_{AB} and the effect of the bias. Notice that, the different intraspecies interaction plays a relevant role because without the interspecies interaction, we would have a binomial-like distribution for type A bosons (slightly repulsive intraspecies interaction, Λ_A) and a catlike state for type B due to an attractive interaction in species B (see Fig. 5(c)). When Λ_{AB} increases (see Fig. 5(d)) or decreases (see Fig. 5(b)) produces an entanglement of the A coefficients maintaining a catlike structure for the B component, until a catlike state between the components A and B is formed. The states of Fig. 5 are present along a vertical line in Figs. 6 and 7 for a fixed value of Λ_B.

In the present case, we have to distinguish between what happens to A and to B since, due to different intraspecies interaction, they are not behaving in the same way. This is reflected in Fig. 6 where we compare several observables for the two components. For the population imbalance of each species, panels (a) and (b), we obtain a
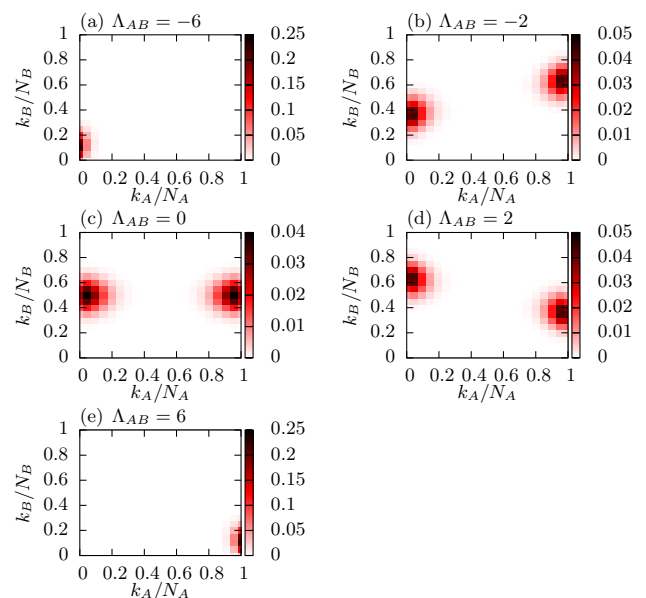
similar description. That type of behaviour was already in Fig. 3 but in the present case the borders between the different regimes become curvy, and the transition zones become wider. This means that for a variation of the parameters Λ_{AB} and Λ_B the state obtained varies more slowly and it is not so sensitive to interaction changes. Another interesting feature is the area around $\Lambda_B = -5$, which is the one explored in Fig. 5, because the difference between species A and B becomes larger. We can see how for $\Lambda_{AB} = 0$, $\Lambda_A = 4$ and $\Lambda_B = -5$ we have A type bosons condensed (see Fig. 6(e)) and B type bosons experimenting the transition. When $|\Lambda_{AB}|$ is increased a transition zone to a condensate for the A bosons appears. Notice that this transition is a consequence of the interspecies interaction. This is observed also for the entropy, the trace of the density matrix squared and the Schmidt gap (see Figs. 7(b), 7(c) and 7(d)). All these facts illustrate the effects of the interspecies interaction.

B. Attractive intraspecies interaction Λ_A

This is the case where there are bosons of type A with attractive intraspecies interaction mixed with bosons B for which we can vary the interaction with themselves and with the other specie.

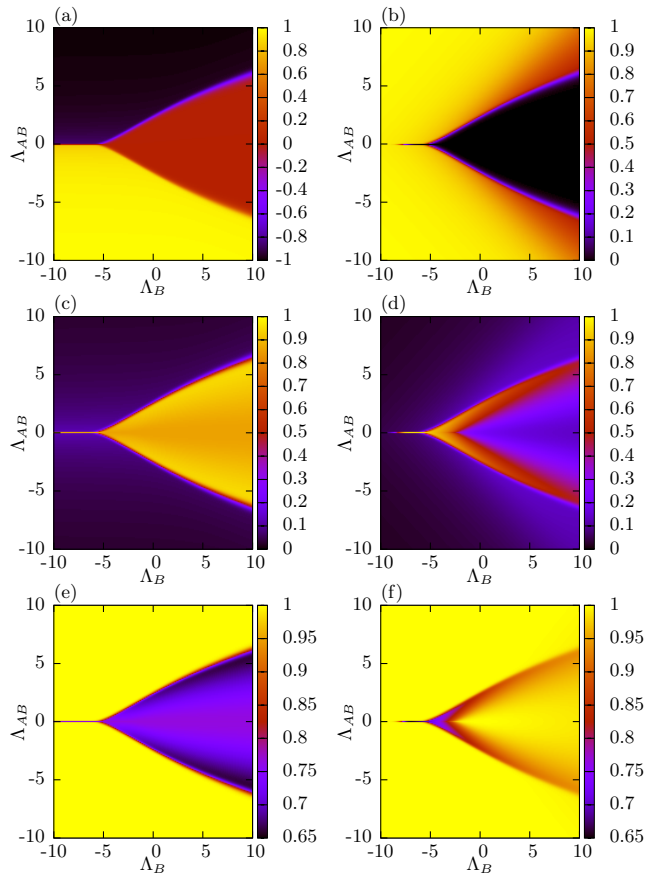In Figs. 8(a) and 8(e) we report the same type of states

FIG. 9: For different intraspecies interaction and fixing $\Lambda_A < 0$ and varying Λ_B and Λ_{AB}, population imbalance of the ground state, z_A, (a) for type A and (b) for type B bosons, z_B. Dispersion of population imbalance of the ground state for each specie, (c) σz_A and (d) σz_B. Condensed fraction of the ground state corresponding to the highest eigenvalue of the one-body density matrix for each type, (e) n_1^A and (f) n_1^B. For all panels $\Lambda_A = -4$, $N_A = N_B = 20$, $J = 20$ and $\epsilon/J = 10^{-10}$.

FIG. 10: For different intraspecies interaction and fixing $\Lambda_A < 0$ and varying Λ_B and Λ_{AB}, (a) difference between the energy of the first excited state and the ground state $\Delta E_{1,0}$. (b) Von Neumann entropy of the ground state for subsystem $A(B)$, $S_{A(B)}$ normalized to its maximum value. (c) Trace of the density matrix squared of the ground state for subsystem $A(B)$, $P_{A(B)}$. (d) Schmidt gap of the ground state for subsystem $A(B)$, $\Delta\lambda^{A(B)}$. For all panels $\Lambda_A = -4$, $N_A = N_B = 20$, $J = 20$ and $\epsilon/J = 10^{-10}$.

found before in Figs. 5(a) and 5(e). For $\Lambda_{AB} = 0$ (see Fig. 8(c)), we have a catlike state for type A bosons and a binomial-like state for type B bosons. This situation is not different from the previous one in Fig. 5 since it corresponds to an exchange of rolls of A and B bosons. However, in Figs. 9 and 10 we can observe this situation from a different point of view because the variable parameter Λ_B corresponds to the species which does the transition from binomial-like to highly localized state whereas for Figs. 6 and 7 bosons of type B experimented the other transition.

On the one hand, for type A bosons we see clearly three zones in Figs. 9(a), 9(c) and 9(e). The top region is the one corresponding to have all bosons of this type on the right (see Fig. 8(e)) so its population imbalance is -1, the dispersion 0 and there is condensation. The bottom region is similar to the top one but with A bosons now confined on the left site (see Fig. 8(a)). The third region located on the right is the one corresponding to the
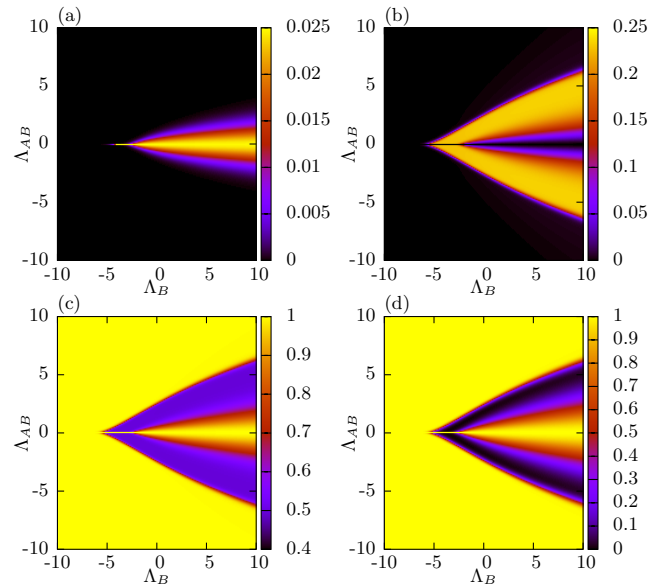
catlike states for the A species. On the other hand, for type B bosons (see Figs. 9(b), 9(d) and 9(f)), the top and the bottom regions are the ones associated respectively with Fig. 8(e) and Fig. 8(a) and the right region is the transition where B bosons pass from being confined in one side, to a catlike state, to a wide peak and finally a binomial-like state for $\Lambda_{AB} = 0$.

In the present case, $\Lambda_A = -4$, we observe large regimes of Λ_B and Λ_{AB} for which there is degeneracy as we can observe in panel (a) of Fig. 10, where we report the energy gap between the ground and the first excited state. Moreover, the last three figures tell us that the presence of catlike states with entanglement, corresponding to the yellow zone in the entropy and purple zone in the trace of the density matrix squared, exists for a wide range of Λ_{AB} (see Figs. 10(b), 10(c) and 10(d)).

VI.   SUMMARY AND CONCLUSIONS

In this master thesis we have discussed the ground state properties of a binary mixture of Bose-Einstein condensates in two spatial sites. The system has been described by means of a two-site two-component Bose-Hubbard Hamiltonian. Taking the same fixed number of particles for each component we have studied the properties of the ground state of the system in different interaction regimes, i.e. varying the intra and interspecies

interactions. The numerical tool used has been a direct diagonalization of the Hamiltonian which is feasible for the small number of particles considered, 20 for each component. In regimes where the interactions are much larger than the tunneling, the analytical ground state of the system can be obtained and can be used as a first approximation to the exact results. We have also considered a regime in which the interactions are of the order of the tunneling. In this case, sizeable quantum correlations are built in the system. First, we have discussed the case in which both components have the same intraspecies interaction, finding quantum correlations arising as the interspecies interaction is tuned. Finally, we have considered a more general case in which both species have a different intraspecies interaction.

New type of states that cannot be found in a single-component condensate have been found and studied as the catlike ones that are of the interest for having entanglement between the two species bosons. We have discussed how the ground state can be characterized and how to differentiate ground state types depending on Λ_A, Λ_B and Λ_{AB} using their properties. We have seen that the population imbalance provides an average information that is complemented with the calculation of its dispersion. To determine the degree of entanglement, it has been shown that the von Neumann entropy gives detailed information about the state whereas the Schmidt gap and the trace of the density matrix squared allow as to have a first approximation view.

[1] C. Gross, T. Zibold, E. Estéve and M.K. Oberthaler. "Nonlinear atom interferometer surpasses classical precision limit". Nature **464**, 1165-1169 (2010).

[2] C. Gross. "Spin squeezing, entanglement and quantum metrology with Bose-Einstein condensates". J. Phys. B: At. Mol. Opt. Phys. **45**, 103001 (2012).

[3] N. Teichmann and C. Weiss. "Coherently controlled entanglement generation in a binary Bose-Einstein condensate". EPL **78**, 10009 (2007).

[4] J.I. Cirac, M. Lewenstein, K. Molmer and P. Zoller. "Quantum superposition states of Bose-Einstein condensates". Phys. Rev. A **57**, 1208 (1998).

[5] R. Gati and M.K. Oberthaler. "A bosonic Josephson junction". J. Phys. B: At. Mol. Opt. Phys. **40**, R61-R89 (2007).

[6] B. Juliá-Díaz, D. Dagnino, M. Lewenstein, J. Martorell and A. Polls. "Macroscopic self-trapping in Bose-Einstein condensates: Analysis of a dynamical quantum phase transition". Phys. Rev. A **81**, 023615 (2010).

[7] M. Melé-Messeguer, Ph.D thesis, *Josephson effect in multicomponent Bose-Einstein condensates*, Universitat de Barcelona (2013).

[8] M. Melé-Messeguer, B. Juliá-Díaz, M. Guilleumas, A. Polls and A. Sanpera. "Weakly linked binary mixtures of $F = 1$ ^{87}Rb BoseEinstein condensates". New J. Phys. **13**, 033012 (2011).

[9] I.I. Satija, R. Balakrishnan, P. Naudus, J. Heward, M. Edwards and C.W. Clark. "Symmetry-breaking and symmetry-restoring dynamics of a mixture of Bose-Einstein condensates in a double well". Phys. Rev. A **79**, 033616 (2009).